PCP
PLANT & CELL PHYSIOLOGY

Structure-Specific Regulation of Nutrient Transport and Metabolism in Arbuscular Mycorrhizal Fungi

Hiromu Kameoka [1,3,*], Taro Maeda [1], Nao Okuma [2] and Masayoshi Kawaguchi [1,2,*]

[1]Division of Symbiotic Systems, National Institute for Basic Biology, 38 Nishigonaka, Myodaiji, Okazaki, Aichi, 444-8585 Japan
[2]The Graduate University for Advanced Studies, 38 Nishigonaka, Myodaiji, Okazaki, Aichi, 444-8585 Japan
[3]Present address: Graduate School of Life and Environmental Sciences, Osaka Prefecture University, 1-1 Gakuen-cho, Naka-ku, Sakai, Osaka, 599-8531 Japan
*Corresponding authors: Hiromu Kameoka, E-mail, thk31601@osakafu-u.ac.jp; Fax, +81-72-254-9472; Masayoshi Kawaguchi, E-mail, masayosi@nibb.ac.jp; Fax, +81-564-55-7564.
(Received March 10, 2019; Accepted June 14, 2019)

Regular Paper

Arbuscular mycorrhizal fungi (AMF) establish symbiotic relationships with most land plants, mainly for the purpose of nutrient exchange. Many studies have revealed the regulation of processes in AMF, such as nutrient absorption from soil, metabolism and exchange with host plants, and the genes involved. However, the spatial regulation of the genes within the structures comprising each developmental stage is not well understood. Here, we demonstrate the structure-specific transcriptome of the model AMF species, *Rhizophagus irregularis*. We performed an ultra-low input RNA-seq analysis, SMART-seq2, comparing five extraradical structures, germ tubes, runner hyphae, branched absorbing structures (BAS), immature spores and mature spores. In addition, we reanalyzed the recently reported RNA-seq data comparing intraradical mycelium and arbuscule. Our analyses captured the distinct features of each structure and revealed the structure-specific expression patterns of genes related to nutrient transport and metabolism. Of note, the transcriptional profiles suggest distinct functions of BAS in nutrient absorption. These findings provide a comprehensive dataset to advance our understanding of the transcriptional dynamics of fungal nutrition in this symbiotic system.

Keywords: Arbuscular mycorrhizal fungi • Metabolism • Transcriptome • Transporter.

Introduction

Arbuscular mycorrhizal fungi (AMF) establish symbiotic relationships with most terrestrial plants (Brundrett and Tedersoo 2018). The central function of these relationships is nutrient exchange, in which AMF supply plants with mineral nutrients and water, in exchange for carbon sources (Roth and Paszkowski 2017). Through this trade, AMF play important roles in terrestrial ecosystems (van der Heijden et al. 1998, van der Heijden et al. 2008), and contribute to an increase in agricultural productivity (Igiehon and Babalola 2017). Therefore, it is important to understand the regulation of nutrient transport and metabolism associated with the symbiotic state of AMF.

Phosphorus and nitrogen are important nutrients absorbed by AMF from soil and then transferred to host plants (Pearson and Jakobsen 1993, Govindarajulu et al. 2005). AMF absorb inorganic phosphate (Pi) from soil using two types of Pi importer, the H^+–Pi symporter and the Na^+–Pi symporter (Harrison and van Buuren 1995, Maldonado-Mendoza et al. 2001, Tisserant et al. 2012, Walder et al. 2016). AMF also utilize organic phosphate by secreting acid phosphatase (Sato et al. 2015). Most of the Pi absorbed by the extraradical mycelium (ERM) is transformed into polyphosphate, presumably in the tonoplast by the vacuolar transporter chaperone (VTC) complex, and then transported to the intraradical mycelium (IRM) through vacuoles (Viereck et al. 2004, Kuga et al. 2008, Tani et al. 2009, Hijikata et al. 2010). Polyphosphate is probably degraded to monophosphate by polyphosphatase and subsequently released from AMF (Capaccio and Callow 1982). Although the mechanism by which AMF release Pi is largely unknown, orthologs of Suppressor of Yeast Gpa1 (SYG1), which share domains with plant and animal Pi exporters, are strong candidates for the Pi exporter (Azevedo and Saiardi 2017, Ezawa and Saito 2018). In the case of nitrogen, AMF absorb NO_3^- and NH_4^+, and transform them into arginine in the ERM. Arginine is transported into the IRM through vacuoles and degraded into NH_4^+ before being transferred to host plants (Govindarajulu et al. 2005, Jin et al. 2005, Cruz et al. 2007, Tian et al. 2010). Many genes which encode transporters and enzymes involved in these processes have been identified (López-Pedrosa et al. 2006, Tian et al. 2010, Pérez-Tienda et al. 2011, Calabrese et al. 2016).

Conversely, AMF strongly depend on plants as their source of carbon (Bago et al. 2000, Roth and Paszkowski 2017), although they have the ability to absorb acetate and monosaccharide on the ERM and germinating spores (Pfeffer et al. 1999, Bago et al. 2000, Helber et al. 2011). AMF acquire monosaccharides by using monosaccharide transporters (MSTs) (Lammers et al. 2001, Helber et al. 2011, Ait Lahmidi et al. 2016) and catabolize them via the glycolytic pathway and tricarboxylic acid cycle (Macdonald and Lewis 1978, Saito 1995). On the other hand, they synthesize trehalose and glycogen to maintain monosaccharide concentrations inside the cells and to transport carbon to the ERM (Shachar-Hill et al. 1995, Bago et al. 2000, Bago et al. 2003). In addition, recent studies have revealed direct lipid transfer from plants to AMF (Jiang et al. 2017, Keymer et al. 2017,

Plant Cell Physiol. 60(10): 2272–2281 (2019) doi:10.1093/pcp/pcz122, Advance Access publication on 26 June 2019, available online at https://academic.oup.com/pcp

Luginbuehl et al. 2017). AMF can elongate and desaturate fatty acids but not synthesize them (Trépanier et al. 2005), because they lack cytosolic fatty acid biosynthesis genes (Wewer et al. 2014, Tang et al. 2016, Kobayashi et al. 2018, Maeda et al. 2018, Sun et al. 2019), indicating that all fatty acids in AMF are plant-derived. The molecular form of transferred lipids is still unknown, but the predicted catalytic properties of the plant enzymes required just before lipid transfer imply that *sn*-2-palmitoylglycerol is a strong candidate (Bravo et al. 2016, Bravo et al. 2017, Jiang et al. 2017, Keymer et al. 2017, Luginbuehl et al. 2017, Brands et al. 2018). AMF produce ATP and synthesize saccharides from fatty acids via the β-oxidation pathway, the glyoxylate cycle and the gluconeogenesis pathway (Bago et al. 1999, Pfeffer et al. 1999, Lammers et al. 2001, Wewer et al. 2014).

As described above, many studies to date have shown the regulation of nutrient transport and metabolism in AMF and the genes involved in these processes. Some of these studies investigated the differences between developmental stages, such as between germinating spores, IRM and ERM. However, the differences between the structures comprising each developmental stage are not well understood. In pre-symbiotic stages, AMF grow curved, thin hyphae called germ tubes from spores (**Fig. 1A**). When the germ tubes attach to host roots, the AMF start to grow IRM and develop arbuscules. As the plant Pi transporters, ammonium transporters and lipid metabolism enzymes required for arbuscular mycorrhizal (AM) symbiosis are specifically expressed in arbuscule-containing cells, it is thought that the transport of phosphorus, nitrogen and lipids occurs in arbuscules (Harrison et al. 2002, Kobae et al. 2010, Yang et al. 2012, Breuillin-Sessoms et al. 2015, Bravo et al. 2017, Keymer et al. 2017, Luginbuehl et al. 2017). The spatial expression patterns of the AMF genes required for nutrient exchange with host plants, however, have not been well examined. Moreover, the site of saccharide transport is still under debate (Fitter 2006, Helber et al. 2011). Although Zeng et al. (2018) recently reported the transcriptome comparing the IRM and arbuscule, the expression patterns of genes putatively related to nutrient exchange have not been analyzed in detail. On the other hand, AMF extend ERM in order to absorb nutrients from soil and produce spores. Straight thick hyphae called runner hyphae are spread out from the root (**Fig. 1B, C**), and subsequently, highly branched hyphae called branched absorbing structures (BAS) differentiate on the runner hyphae (**Fig. 1B, C**) (Bago et al. 1998a). Daughter spores are formed on the BAS, and gradually mature (**Fig. 1B, D**) (Bago et al. 1998a). The features of each extraradical structures, responsible for nutrient absorption and metabolism, are completely unknown. Previous studies speculated that the BAS have important roles for nutrient absorption because of their cytological similarity with arbuscules and because the pH decrease of the media around the BAS forming spores may be associated with Pi absorption (Li et al. 1991, Bago et al. 1998a, bago et al. 1998b). However, there is no direct evidence to show nutrient absorption by the BAS. Several studies have reported transcriptome analyses comparing the ERM with the IRM or germinating spores (Tisserant et al. 2012, Tisserant et al. 2013, Kikuchi et al. 2014, Tsuzuki et al. 2016), but to our knowledge, there are no reports that comprehensively investigate the spatial gene expression pattern among extraradical structures.

Here, we show the structure-specific transcriptome of the model AMF species, *Rhizophagus irregularis*. We collected five individual extraradical structures (germ tubes, runner hyphae, BAS, immature spores and mature spores) from an in vitro hairy root-AMF co-culture system (Tsuzuki et al. 2016). This enabled us to grow AMF under defined environmental conditions and to collect each structure with minimal damage. We then performed RNA-seq analysis on the structures. To overcome the low volume of sample available, we applied the SMART-seq2 method, in which we were able to construct RNA-seq libraries from as little as 10 pg of RNA (Picelli et al. 2013, Picelli et al.

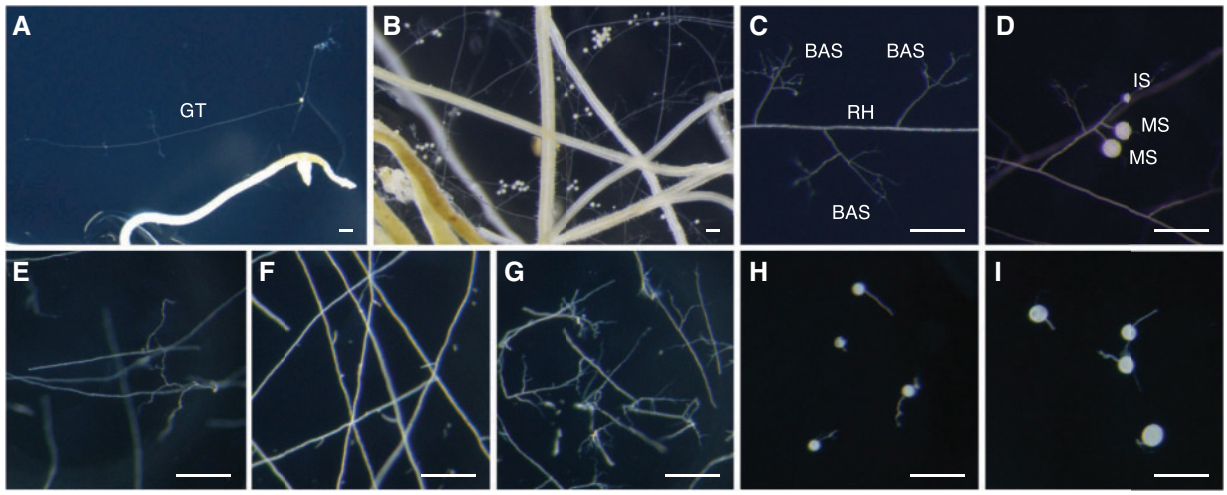

Fig. 1 Extraradical structures. (A) One-week-cultured *R. irregularis* in the pre-symbiotic stage. (B–D) Six-week-cultured *R. irregularis* in the symbiotic stage; global view (B), runner hyphae and BAS (C) and immature and mature spores (D). (E–I) Samples for RNA-seq analysis; germ tubes (E), runner hyphae (F), BAS (G), immature spores (H) and mature spores (I). Bar = 200 μm. GT, germ tubes; RH, runner hyphae; BAS, branched absorbing structures; IS, immature spores; MS, mature spores.

2014). In addition, we reanalyzed the most recent RNA-seq data comparing IRM and arbuscule (Zeng et al. 2018), focusing on the genes possibly involved in nutrient exchange. Our analyses captured the distinct features of each structure and revealed structure-specific expression patterns of genes related to nutrient transport and metabolism. These results provide a basic dataset to help us understand fungal nutrition in this symbiotic system.

Results and Discussion

Structure-specific transcriptome analysis of *R. irregularis* using the low input RNA-seq method

To investigate the physiological features of extraradical structures of AMF, we performed transcriptome analysis in *R. irregularis* DAOM197198, comparing five extraradical structures, germ tubes, runner hyphae, BAS, immature spores and mature spores (Fig. 1E–I). Although samples of the runner hyphae, immature spores and mature spores contained small amounts of the BAS (Fig. 1F, H, I), we believe that the influence of the contamination was negligible, because the amount of RNA extracted from the BAS was much lower than that from other structures (Supplementary Table S1). As it was difficult to collect sufficient amounts of samples for the regular RNA-seq method, we constructed the RNA-seq libraries using the SMART-seq2 method, a low input library preparation method (Picelli et al. 2013, Picelli et al. 2014). The libraries were sequenced using the Illumina HiSeq1500 and the reads obtained were analyzed based on the latest genome data (Maeda et al. 2018) (Supplementary Table S2).

We first validated the sampling and sequencing method by using principal component analysis (PCA) of gene expression profiles among structures and replicates (Fig. 2A). PC1 clearly discriminated between hyphae and spores, while PC2 captured the maturation of spores. Although hyphae samples were not clearly separated in the PC1–PC2 plane, they were separated in the PC3–PC4 plane. These results indicated that the low input RNA-seq method successfully detected the differences in gene expression patterns among the extraradical structures.

Among the 19,918 genes expressed in all the samples, 1,977 genes were differentially expressed among the extraradical structures (Supplementary Table S3). To visualize the expression pattern of the differentially expressed genes (DEGs), we again performed PCA. The axes of the five structures indicated that PC1 demonstrates whether the DEGs were expressed in hyphae or spores and that PC2 demonstrates whether they were expressed in pre-symbiotic hyphae, germ tubes, or symbiotic extraradical hyphae, runner hyphae and BAS (Fig. 2B). This result seems reasonable considering the functional similarity of the structures.

DEGs were densely mapped near the axis of each structure, showing that many DEGs were highly expressed in one structure only (Fig. 2B). Therefore, we classified the DEGs into five clusters using the K-means method. Clusters 1, 2, 3, 4 and 5 were represented by genes highly expressed in the germ tubes, runner hyphae, BAS, immature spores or mature spores, respectively (Fig. 2B, C). To investigate the function of genes in each cluster, we performed gene ontology (GO) enrichment analysis using the GO term Biological Process (Supplementary Table S4). In cluster 3, the GO term 'transmembrane transport' (GO: 0055085) was enriched. Although called 'branching absorbing structures', there is no direct evidence to show nutrient absorption by the BAS (Bago et al. 1998a, bago et al. 1998b); however, our result supports the hypothesis that BAS is involved in nutrient absorption. The enrichment of many GO terms involved in DNA replication and nuclear cell division in cluster 4 appears to reflect the burst in mitosis that occurs during spore maturation (Marleau et al. 2011). Thus, the results of the GO enrichment analysis are consistent with previous observations, suggesting that our RNA-seq analysis captured the characteristic transcriptional profiles of each structure.

Survey of genes related to nutrient transport and metabolism

To date, many studies have identified the genes related to nutrient transport and metabolism in *R. irregularis*. These genes, however, have been annotated based on past transcriptome or genome data and are sometimes named differently in different reports (e.g. *GiPT* in Maldonado-Mendoza et al. 2001 and *RiPT1* in Walder et al. 2016). Therefore, we re-annotated these genes based on our current genome data (Maeda et al. 2018), and renamed them uniformly, using the reported gene names (Supplementary Table S5). In addition, we searched unidentified genes, putatively related to nutrient transport and metabolism, based on orthology with the genes of *Saccharomyces cerevisiae* or *Aspergillus nidulans*, as detected by the OrthoFinder software (Emms and Kelly 2015, Maeda et al. 2018) (Supplementary Table S5). Next, we examined the expression patterns of these genes, as discussed below.

Absorption and metabolism of mineral nutrients

Two of three genes encoding H^+–Pi symporters, *PT1* (*GiPT* in Maldonado-Mendoza et al. 2001 and *RiPT1* in Walder et al. 2016) and *PT2*, were differentially expressed among the extraradical structures, while *PT3* and two genes encoding Na^+–Pi symporters, *PT5* and *PT6*, were not differentially expressed and showed relatively low expression levels (Fig. 3A, Supplementary Table S5). *PT1* was the most highly expressed gene among the Pi transporters and showed the highest expression level in the BAS (Fig. 3A), suggesting the importance of the BAS for Pi absorption. Expression of *ACP1*, a gene encoding extracellular acid phosphatase, was increased with the formation of the immature spores from BAS, and reached the maximum in the mature spores (Fig. 3B). The mineralization of organic phosphate by ACP1 around the BAS may enhance Pi absorption (Ezawa and Saito 2018). *VTC1*, which is thought to be involved in Pi polymerization, was highly expressed in the runner hyphae, while *PPN3*, a gene encoding endopolyphosphatase, was highly expressed in the BAS (Fig. 3C, D). These results imply that runner hyphae and the BAS have distinct functions in Pi metabolism. The expression levels of *SYG1* orthologs were low in the extraradical structures (Supplementary Table S5).

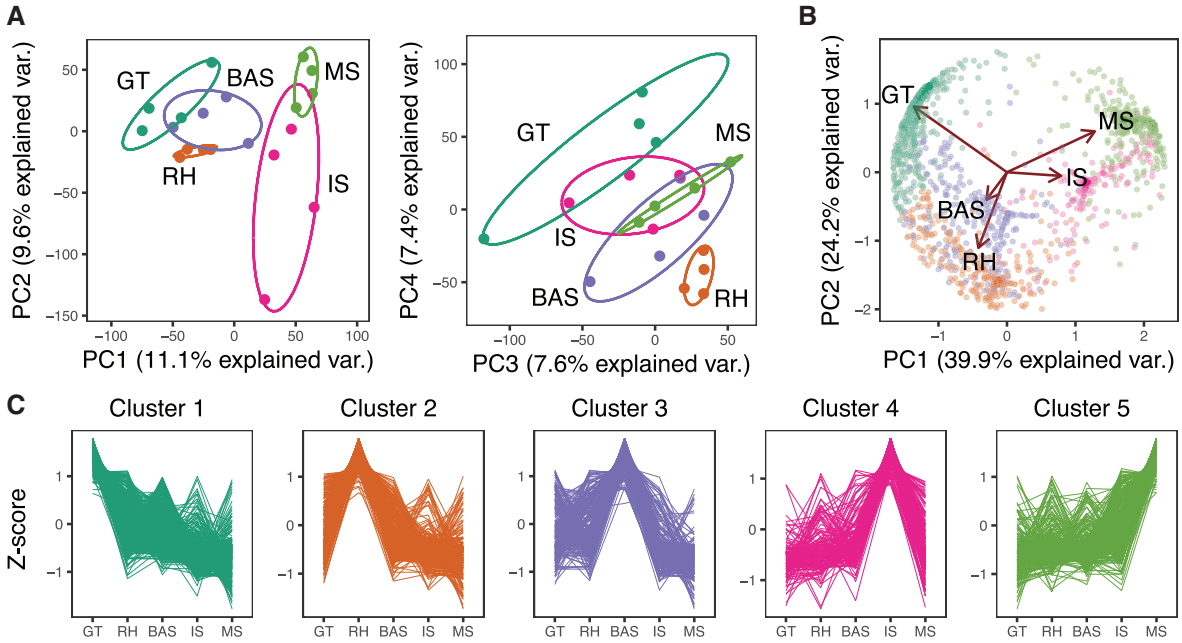

Fig. 2 Detection of structure-specific gene expression. (A) PCA of gene expression profiles between structures and replicates. Ellipses represent a 68% confidence region for each structure. (B) PCA analysis of 1,977 differentially expressed genes (DEGs). DEGs were classified into five clusters using the K-means method. (C) The scaled expression levels of genes in each cluster. Genes in the same clusters are labeled in the same color. GT, germ tubes; RH, runner hyphae; BAS, branched absorbing structures; IS, immature spores; MS, mature spores.

The expression of *AMT1* was dominant in the extraradical structures among ammonium transporters (Fig. 3E). *AMT1* was expressed at relatively high levels in all structures examined, especially in the BAS (Fig. 3E). The expression of genes encoding glutamine synthase, the first step in ammonium assimilation, was highest in the germ tubes (Fig. 3F). Considering the expression pattern of these genes, AMF may use ammonium as a nitrogen source in all life stages. Conversely, genes encoding nitrate transporter, nitrate reductase and nitrite reductase were highly expressed in the runner hyphae while strongly suppressed in the germ tubes (Fig. 3G–I), suggesting that runner hyphae have a central role in nitrate metabolism and that *R. irregularis* can utilize nitrate, as well as ammonium, in the symbiotic stages. As the reduction of nitrate to ammonium requires high energy (Courty et al. 2015), it seems reasonable that the AMF assimilate nitrate in the symbiotic stages only, where they can obtain sufficient carbon sources from host plants. The expression patterns of the genes encoding urea transporter and urease were similar to those of nitrate-related genes (Fig. 3J, K). Some arginine metabolism genes were differentially expressed among the extraradical structures, but their expression did not follow a particular pattern (Supplementary Table S5).

One of three genes encoding aquaporin, *AQP1*, was expressed specifically in the immature spores (Fig. 3L). As AQY1, a yeast spore-specific aquaporin, may function in spore maturation (Sidoux-Walter et al. 2004), *AQP1* might also be involved in this process. Genes encoding iron transporter, zinc transporter, copper-exporting ATPase and sulfate transporter were also differentially expressed among the extraradical structures (Fig. 3M–P).

Carbon absorption and metabolism

Consistent with the previous observation that AMF can absorb acetate and monosaccharide from the ERM (Pfeffer et al. 1999, Helber et al. 2011), the expression of acetate transporters, carboxylate transporters and MSTs was clearly detected in the extraradical structures (Fig. 4A–C). As our previous phylogenetic analysis did not classify *RiMST6* (Ait Lahmidi et al. 2016) into the orthogroup of MSTs (OG0000019) but into that of carboxylate transporters (OG0001862) (Maeda et al. 2018), we renamed it *JEN2* (Supplementary Table S5). MST2 is a monosaccharide transporter which is expressed in the IRM and required for mycorrhiza formation involving arbuscule development (Helber et al. 2011). While expression of *MST2* in the ERM was not detected previously (Helber et al. 2011), a relatively low but clear level of expression was observed in the BAS (Fig. 4A). In the extraradical structures, *MST4* and *MST5* showed relatively high expression levels among the *MSTs* (Fig. 4A), suggesting the contribution of these genes to monosaccharide absorption in the ERM. *ACT2* and *ACT3*, genes encoding acetate transporter, were expressed in a broad range of the extraradical structures (Fig. 4B). On the other hand, the expression of *JEN3* and *JEN4*, genes encoding carboxylate transporters, were significantly highly expressed in the BAS (Fig. 4C), suggesting the potential of the BAS for carboxylate absorption.

Two of seven genes encoding fatty-acid-CoA ligase, *FAL6* and *FAL7*, which functions in the β-oxidation pathway, were differentially expressed with statistical significance, and showed the highest expression levels in the germ tubes (Fig. 4D). In addition, both of the genes encoding glyoxylate

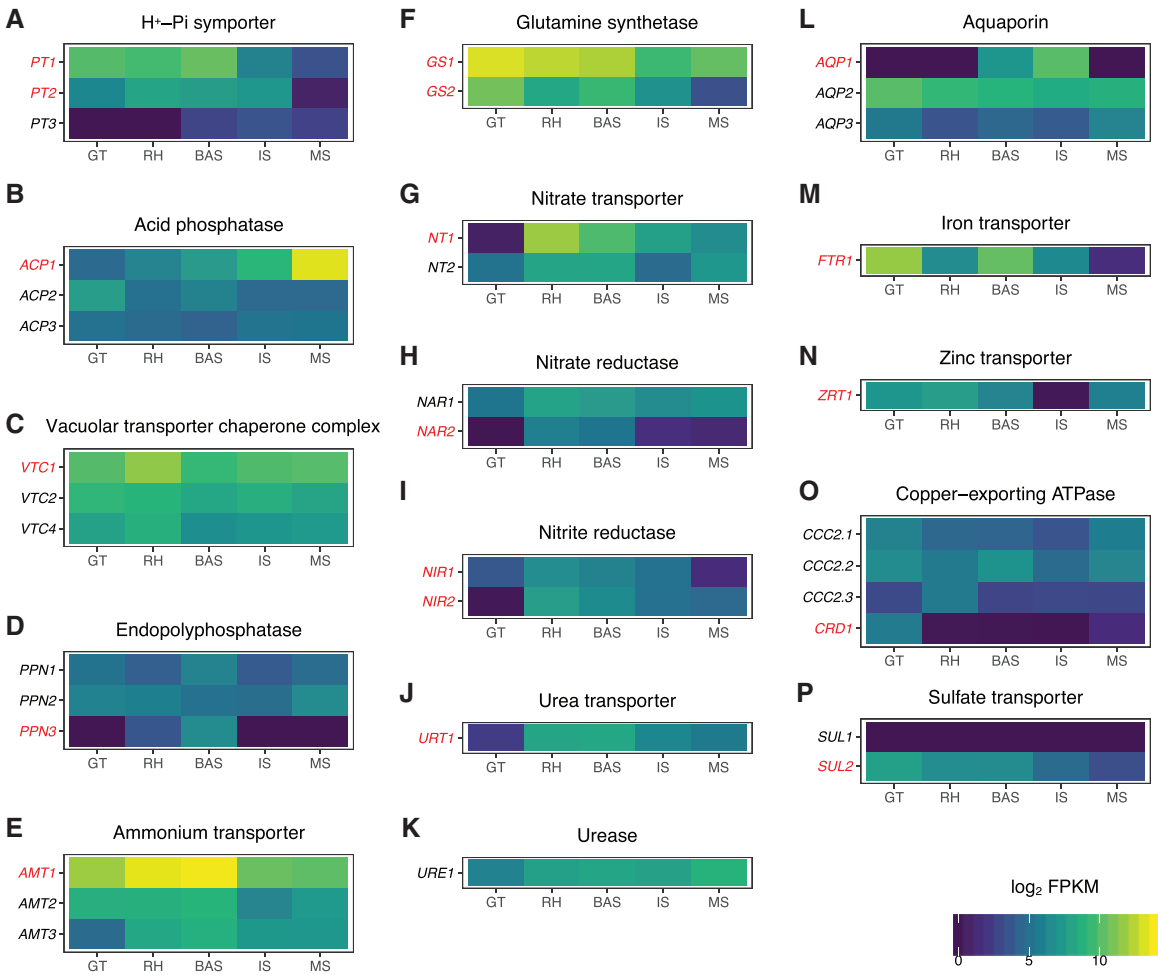

Fig. 3 Expression patterns of genes related to mineral nutrient absorption and metabolism. Log_2 fragments per kilobase of exon per million reads mapped (FPKM) in each structure of the genes encoding H^+–Pi symporter (A), acid phosphatase (B), VTC complex (C), endophosphatase (D), ammonium transporter (E), glutamine synthase (F), nitrate transporter (G), nitrate reductase (H), nitrite reductase (I), urea transporter (J), urease (K), aquaporin (L), iron transporter (M), zinc transporter (N), copper-exporting ATPase (O) and sulfate transporter (P). The expression of genes in red letters was statistically significantly different among the structures (false discovery rate; FDR < 0.05). GT, germ tubes; RH, runner hyphae; BAS, branched absorbing structures; IS, immature spores; MS, mature spores.

cycle-specific enzymes, isocitrate lyase and malate synthase, were significantly highly expressed in the germ tubes (Fig. 4E, F). Genes encoding phosphoenolpyruvate carboxykinase, an enzyme functioning in gluconeogenesis, were also highly expressed in the germ tubes, although the differences were not statistically significant (Fig. 4G). These expression patterns are consistent with reports that most of the carbon storage in the spores of AMF is in the form of lipids and fatty acids (Jabaji-Hare 1988, Bécard et al. 1991). Conversely, two genes encoding enzymes for the modification of fatty acids, fatty acid elongase and delta 9-fatty acid desaturase, were highly expressed in the mature spores (Fig. 4H, I). These genes might have an important contribution to fatty acid storage in spores. On the other hand, the gene encoding trehalase was highly expressed in the runner hyphae (Fig. 4J), presumably reflecting the abundant saccharides available from host plants in the symbiotic stages.

Nutrient exchange with host plants in the intraradical phase

Although Zeng et al. (2018) provided high quality RNA-seq data comparing the IRM and arbuscule, there are no reports of the detailed analyses of genes related to nutrient exchange. To investigate the function of IRM and arbuscule in nutrient exchange between AMF and host plants, we reanalyzed the RNA-seq data. PCA between samples clearly discriminated between the IRM and arbuscule samples (Fig. 5A).

We then analyzed DEGs between the IRM and arbuscule. Among the phosphate-related genes examined (Supplementary Table S5), *PPN3*, a gene encoding endophosphatase, and *SYG1-1*, a gene encoding the homolog of a Pi exporter, were mainly expressed in the arbuscules compared to the IRM (Fig. 5B, C). Although the functions of these genes have not been investigated, it is possible that they are involved in Pi release from AMF. In concordance with the report that

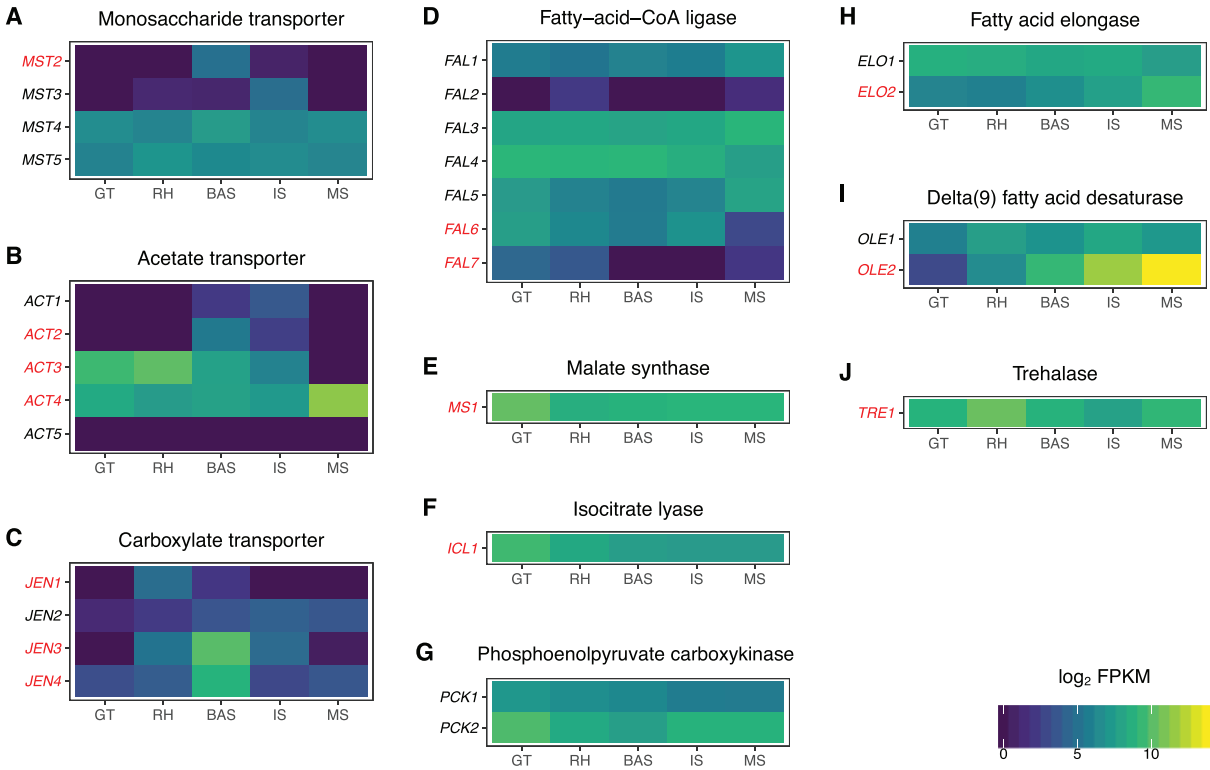

Fig. 4 Expression patterns of genes related to carbon absorption and metabolism. Log_2 fragments per kilobase of exon per million reads mapped (FPKM) in each structure of the genes encoding monosaccharide transporter (A), acetate transporter (B), carboxylate transporter (C), fatty-acid-CoA ligase (D), malate synthase (E), isocitrate lyase (F), phosphoenolpyruvate carboxykinase (G), fatty acid elongase (H), delta 9-fatty acid desaturase (I) and trehalase (J). The expression of genes in red letters was statistically significantly different among the structures (FDR < 0.05). GT, germ tubes; RH, runner hyphae; BAS, branched absorbing structures; IS, immature spores; MS, mature spores.

arginine is degraded into ammonium before nitrogen is transferred to host plants (Jin et al. 2005), urease, which catalyzes the conversion of urea to ammonium in the final step of arginine degradation, was highly expressed in the arbuscules (Fig. 5D). *CRD1*, a gene encoding copper-exporting ATPase, and *FTR1*, a gene encoding an iron transporter, were also highly expressed in the arbuscules (Fig. 5E, F), suggesting a function for arbuscules in copper and iron exchange between plants and AMF. Although *MST2* was expressed in both the IRM and arbuscules, its expression level was higher in the arbuscules (Fig. 5G), suggesting that arbuscules have a significant role in saccharide absorption. While *ACT1*, *ACT2* and *ACT3* showed lower expression levels in extraradical structures among genes encoding acetate transporter (Fig. 4B), their expression levels were significantly high in arbuscules (Fig. 5H). On the other hand, two carboxylate transporters, *JEN3* and *JEN4*, which were significantly expressed in the BAS (Fig. 4C), also showed higher expression levels in the arbuscules compared to the IRM with statistical significance (Fig. 5I). The expression of some genes encoding acetate transporters and carboxylate transporters was also induced in the arbuscules (Fig. 5H, I). Two lipid metabolism-related genes *MGL1* and *OLE2*, which encode monoacylglyceride lipase and delta 9-fatty acid desaturase, respectively, were highly expressed in the arbuscules (Fig. 5J, K). This result led us to hypothesize that *sn*-2-palmitoylglycerol is hydrolyzed into palmitic acid and glycerol by MGL1, and palmitic acid is desaturated by OLE2. Thus, analysis of the expression patterns of putative genes related to nutrient exchange has provided insight into the function of arbuscules for nutrient exchange between AMF and host plants.

Conclusion

In this study, we performed transcriptome analysis comparing extraradical structures of the AMF *R. irregularis* to investigate the functions of these structures in nutrient absorption and metabolism. Our analysis generated structure-specific transcriptional profiles and detected DEGs among the structures. Further analysis of genes related to nutrient transport and metabolism, and reannotation using the latest genome data, revealed the characteristic functions of each structure; e.g. fatty acid consumption in the germ tubes (Fig. 4D–G), nitrate absorption and reduction in the runner hyphae (Fig. 3F–I), Pi, ammonium and carboxylate absorption in the BAS (Fig. 3A, E; Fig. 4C), and fatty acid modification in the mature spores (Fig. 4H, I). In addition, we reanalyzed the RNA-seq data comparing the IRM and arbuscule (Zeng et al. 2018) and detected the expression of putative genes related to nutrient exchange in the arbuscule (Fig. 5). Although many studies have revealed the regulation of nutrient transport and metabolism by AMF, the

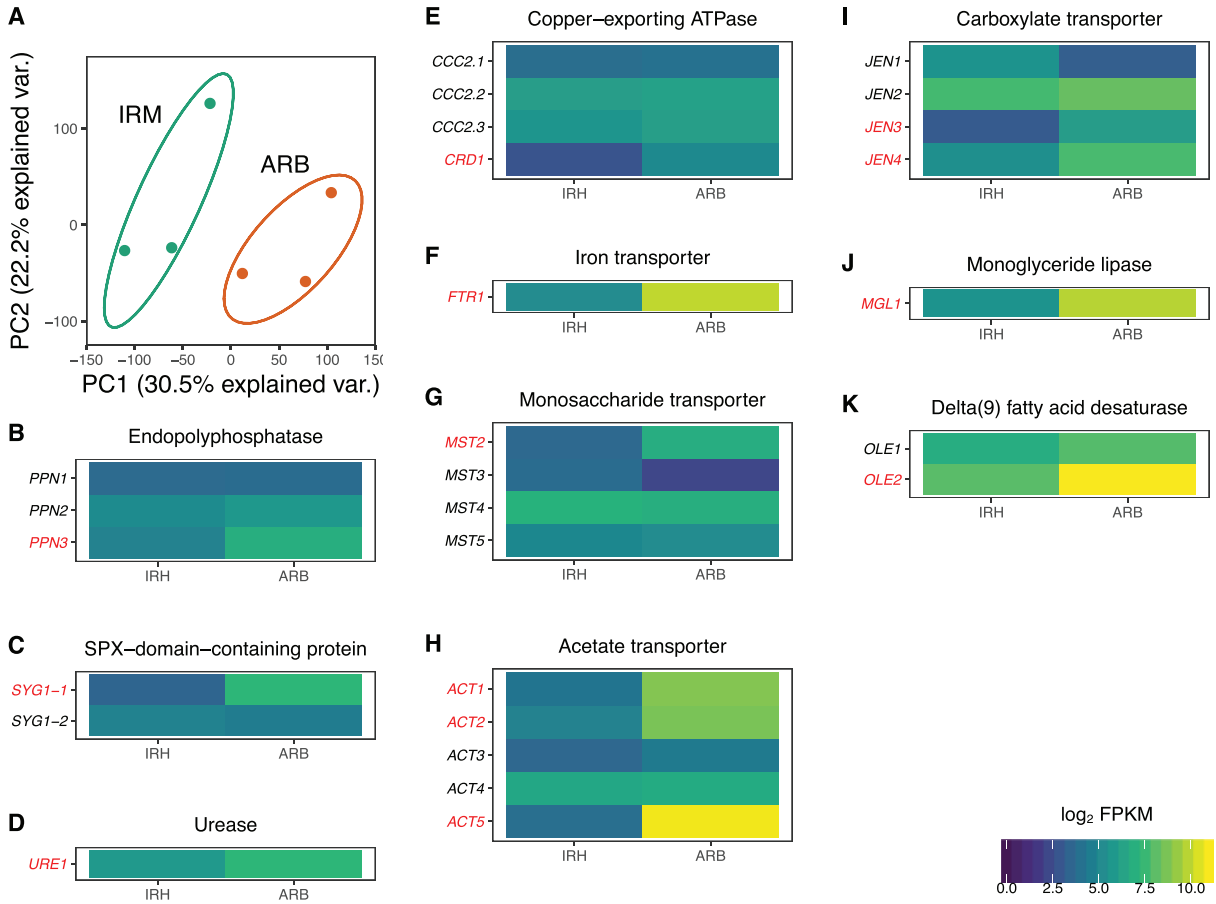

Fig. 5 Differentially expressed genes between IRM and ARB. (A) PCA of gene expression profiles of IRM and arbuscule samples. (B–K) Log_2 fragments per kilobase of exon per million reads mapped (FPKM) in intraradical mycelia or arbuscules of the genes encoding endophosphatase (B), SPX-domain-containing protein (C), urease (D), copper-exporting ATPase (E), iron transporter (F), acetate transporter (G), monosaccharide transporter (H), carboxylate transporter (I), monoglyceride lipase (J) and delta 9-fatty acid desaturase (K). The expression of genes in red letters was statistically significantly different between the IRM and ARB (FDR < 0.05). IRM, intraradical mycelium; ARB, arbuscule.

spatial regulations among the structures have remained largely unknown. Our data, therefore, provide comprehensive information for understanding the dynamics of nutrient regulation in this symbiotic system.

Of note, our results suggest distinctive functions between runner hyphae and BAS for nutrient absorption and metabolism. Although they have morphological differences, it was not clear previously as to whether the runner hyphae and BAS have different transcriptional profiles, because they are not separated by either a cell membrane nor a cell wall and share a common cytoplasm (Bago et al. 1998a). This question had not been approached previously, probably because of technical difficulties. Our RNA-seq analysis using the SMART-seq2 method clearly illustrated the difference in the transcriptome between the two structures. Although many genes related to nutrient absorption and metabolism were expressed in both structures, they showed distinctive expression patterns, suggesting the importance of the runner hyphae for the absorption and reduction of nitrate (**Fig. 3G–I**) and that of the BAS for the absorption of Pi, ammonium and carboxylate (**Figs. 3A, E, 4C**). These results provide a new perspective for investigating nutrient absorption and metabolism in AMF.

In order to avoid damage as much as possible during sampling, we used an in vitro hairy root-AMF co-culture system (Tsuzuki et al. 2016) to analyze gene expression in extraradical structures. As this system is an artificial one that does not use mycorrhiza of intact plants, we are aware that the patterns of gene expression may be different to those observed when AMF colonize intact roots in soil. In situ hybridization analysis might be an effective strategy for the future, to confirm the gene expression patterns in the structures of AMF that colonize intact plants. On the other hand, our system allows us to modify environmental conditions, such as nutrient composition. Knowledge of the regulation of fungal gene expression under various conditions is important in understanding nutrient transport and metabolism in AM symbiosis in nature. Our data provide a basic reference for examining the environmental responses of AMF. To further understand the physiological functions of each structure, functional analysis of DEGs is required. Host-induced gene silencing and virus-induced gene silencing, which are able to silence the genes of AMF in the IRM

by using dsRNA produced by the host plant or a virus to infect the host plant, respectively (Helber et al. 2011, Kikuchi et al. 2016, Tsuzuki et al. 2016), will be useful tools for the analysis of the putative genes related to nutrient exchange expressed in arbuscules. However, no method to manipulate gene expression in extraradical structures currently exists. Establishment of new technologies for transformation, gene silencing in extraradical structures and mutagenesis is therefore necessary.

In addition to absorption and metabolism of nutrients, extraradical structures have important functions such as infection in host plants, interaction with associated bacteria and spore formation, the genetics of which have been poorly investigated. Our data provide fundamental information which should assist in these investigations.

Materials and Methods

Biological materials and growth conditions

Hairy roots of carrot (*Daucus carota*) generated in Tsuzuki et al. (2016) were grown on M medium (731 mg l^{-1} $MgSO_4 \cdot 7H_2O$, 80 mg l^{-1} KNO_3, 65 mg l^{-1} KCl, 4.8 mg l^{-1} KH_2PO_4, 288 mg l^{-1} $Ca(NO_3)_2 \cdot 4H_2O$, 10 g l^{-1} Sucrose, 8 mg l^{-1} NeFeEDTA, 0.75 mg l^{-1} KI, 6 mg l^{-1} $MnCl_2 \cdot 4H_2O$, 2.65 mg l^{-1} $ZnSO_4 \cdot 7H_2O$, 1.5 mg l^{-1} H_3BO_3, 0.13 mg l^{-1} $CuSO_4 \cdot 5H_2O$, 0.0024 mg l^{-1} $Na_2MoO_4 \cdot 2H_2O$, 3 mg l^{-1} glycine, 0.1 mg l^{-1} thiamine hydrochloride, 0.1 mg l^{-1} pyridoxine hydrochloride, 0.5 mg l^{-1} nicotinic acid, 50 mg l^{-1} myo inositol, 4 g l^{-1} gelrite) (Bécard and Fortin 1988) at 28°C in the dark. Monoxenic cultures of the hairy root and *R. irregularis* DAOM 197198 (Premier Tech, Rivière-du-Loup, Canada) were performed as described in Tsuzuki et al. (2016).

Sample preparation and RNA extraction

Extraradical structures were dissected using a surgical knife under a stereoscopic microscope. To avoid wounding stress responses, dissected structures were frozen within *ca.* 1 min in liquid nitrogen. After being crushed in RNA extraction buffer, sufficient quantity of structures for one of the four replicates were gathered into a tube. Germ tubes were sampled from 7 days after inoculation (dai) monoxenic culture plates. The hyphae from 10–30 germinating spores which did not attach to the hairy root were collected as one of the four replicates. We collected 20–50 BAS which did not contain spores, 5–10 runner hyphae (10 BAS were dissected from each runner hyphae), five immature spores and five mature spores as one of the four replicates from 42 dai plates. As the runner hyphae and BAS were dissected from the base of the BAS, the BAS samples did not include the runner hyphae, while the runner hyphae included small amount of the BAS. Spores smaller than 100 μM in diameter were defined as immature spores, while the larger ones (>100 μM in diameter) were defined as mature spores. RNA was extracted using a NucleoSpin RNA XS kit (Macherey-Nagel, Düren, Germany). Since the amount of RNA extracted from spores was often too much to amplify in the same cycle as that from hyphal samples, between 2 and 100% of extracted RNA from spores was used. The number of samples used to synthesize cDNA is summarized in Supplementary Table S1.

Library synthesis and sequencing

RNA was reverse-transcribed and amplified using the SMART-Seq v4 Ultra Low Input RNA Kit for Sequencing (Clontech, Mountain View, CA, USA) (Picelli et al. 2013, Picelli et al. 2014). The quality and the quantity of cDNA was checked using the Agilent 2100 Bioanalyzer with the High Sensitivity DNA kit (Agilent Technologies, Santa Clara, CA, USA). cDNA was sheared using the COVARIS S2 system (Covaris Inc., Woburn, MA, USA) and converted to RNA-seq libraries using the low input library prep kit (Clontech, Mountain View, CA, USA). Each library was diluted to 2 nM. Four replicates were prepared for each structure. Details for each cDNA library are summarized in Supplementary Table S1. A total of 102 bp single-end reads were obtained using the HiSeq 1500 (Illumina, San Diego, CA, USA). Raw sequence data has been deposited in the DDBJ Sequence Read Archive (DRA) under BioProject PRJDB6136. The RNA-seq data comparing the IRM and arbuscule were obtained from BioProject PRJNA389248.

DEG analysis

These reads were trimmed using Trimmomatic (v0.33) (Bolger et al. 2014). Trimmed reads were mapped to the latest genome data (Maeda et al. 2018) by using tophat2 (v2.1.0) (Kim et al. 2013). The read counts were calculated by HT-seq (v0.6.1) (Anders et al. 2015). Information about raw reads, trimming and mapping are summarized in Supplementary Table S2. DEGs ($|\log_2 FC| > 1$, FDR < 0.05) were detected using EdgeR-robust (v3.18.1) (Robinson et al. 2010, Zhou et al. 2014). To compare the expression profiles among structures, count per million (CPM) of each gene was normalized by trimmed-mean-of-M-values (TMM) using edgeR (Robinson et al. 2010), and subsequently scaled using the scale function in R (v3.4.1). PCA was performed using the prcomp function in R, using all expressed genes. Non-expressed genes were eliminated from this analysis. For PCA comparing the DEGs, the expression levels of DEGs in each structure calculated by EdgeR-robust were scaled using the scale function in R and PCA was performed using the prcomp function in R. K-means classification of DEGs was performed using the kmeans function in R. Gene ontology was annotated by Blast2GO (v4.1) (Conesa et al. 2005). Enrichment analyses were performed by goseq (Young et al. 2010).

Supplementary Data

Supplementary data are available at PCP online.

Funding

The Japan Science and Technology Agency [ACCEL JPMJAC1403 to M.K.].

Acknowledgments

We thank Dr. Syusaku Tsuzuki, Dr. Naoya Takeda, Dr. Katsuharu Saito and Prof. Tatsuhiro Ezawa for their critical suggestions and Ms. Yuko Ogawa, Ms. Sachiko Tanakta, Ms. Asami Tokairin and Ms. Yumi Yoshinori for their experimental support. We appreciate Dr. Katsushi Yamaguchi, Prof. Shuji Shigenobu, Functional Genomics Facility and Data Integration and Analysis Facility, NIBB Core Research Facilities for their technical support.

Disclosures

The authors have no conflicts of interest to declare.

References

Ait Lahmidi, N., Courty, P.E., Brulé, D., Chatagnier, O., Arnould, C. and Doidy, J. (2016) Sugar exchanges in arbuscular mycorrhiza: RiMST5 and RiMST6, two novel *Rhizophagus irregularis* monosaccharide transporters, are involved in both sugar uptake from the soil and from the plant partner. *Plant Physiol. Biochem.* 107: 354–363.

Anders, S., Pyl, P.T. and Huber, W. (2015) HTSeq—a Python framework to work with high-throughput sequencing data. *Bioinformatics* 31: 166–169.

Azevedo, C. and Saiardi, A. (2017) Eukaryotic phosphate homeostasis: the inositol pyrophosphate perspective. *Trends Biochem. Sci.* 42: 219–231.

Bago, B., Azcón-Aguilar, C., Goulet, A. and Piché, Y. (1998a) Branched absorbing structures (BAS): a feature of the extraradical mycelium of symbiotic arbuscular mycorrhizal fungi. *New Phytol.* 139: 375–388.

Bago, B., Azcón-Aguilar, C. and Piché, Y. (1998b) Architecture and developmental dynamics of the external mycelium of the arbuscular mycorrhizal fungus *Glomus intraradices* grown under monoxenic conditions. *Mycologia* 90: 52–62.

Bago, B., Pfeffer, P.E., Abubaker, J., Jun, J., Allen, J.W., Brouillette, J., et al. (2003) Carbon export from arbuscular mycorrhizal roots involves the translocation of carbohydrate as well as lipid. *Plant Physiol*. 131: 1496–1507.

Bago, B., Pfeffer, P.E., Douds, D.D., Jr., Brouillette, J., Bécard, G. and Shachar-Hill, Y. (1999) Carbon metabolism in spores of the arbuscular mycorrhizal fungus *Glomus intraradicesas* revealed by nuclear magnetic resonance spectroscopy. *Plant Physiol.* 121: 263–272.

Bago, B., Pfeffer, P.E. and Shachar-Hill, Y. (2000) Carbon metabolism and transport in arbuscular mycorrhizas. *Plant Physiol.* 124: 949–957.

Bécard, G., Doner, L.W., Rolin, D.B., Douds, D.D. and Pfeffer, P.E. (1991) Identification and quantification of trehalose in vesicular-arbuscular mycorrhizal fungi by *in vivo* 13C NMR and HPLC analyses. *New Phytol.* 118: 547–552.

Bécard, G. and Fortin, J.A. (1988) Early events of vesicular–arbuscular mycorrhiza formation on Ri T-DNA transformed roots. *New Phytol.* 108: 211–218.

Bolger, A.M., Lohse, M. and Usadel, B. (2014) Trimmomatic: a flexible trimmer for Illumina sequence data. *Bioinformatics* 30: 2114–2120.

Brands, M., Wewer, V., Keymer, A., Gutjahr, C. and Dörmann, P. (2018) The *Lotus japonicus* acyl-acyl carrier protein thioesterase FatM is required for mycorrhiza formation and lipid accumulation of *Rhizophagus irregularis*. *Plant J.* 95: 219–232.

Bravo, A., Brands, M., Wewer, V., Dörmann, P. and Harrison, M.J. (2017) Arbuscular mycorrhiza-specific enzymes FatM and RAM2 fine-tune lipid biosynthesis to promote development of arbuscular mycorrhiza. *New Phytol.* 214: 1631–1645.

Bravo, A., York, T., Pumplin, N., Mueller, L.A. and Harrison, M.J. (2016) Genes conserved for arbuscular mycorrhizal symbiosis identified through phylogenomics. *Nat. Plants* 2: 15208.

Breuillin-Sessoms, F., Floss, D.S., Gomez, S.K., Pumplin, N., Ding, Y., Levesque-Tremblay, V., et al. (2015) Suppression of arbuscule degeneration in *Medicago truncatula phosphate transporter4* mutants is dependent on the ammonium transporter 2 family protein AMT2; 3. *Plant Cell* 27: 1352–1366.

Brundrett, M.C. and Tedersoo, L. (2018) Evolutionary history of mycorrhizal symbioses and global host plant diversity. *New Phytol.* 220: 1108–1115.

Calabrese, S., Pérez-Tienda, J., Ellerbeck, M., Arnould, C., Chatagnier, O., Boller, T., et al. (2016) GintAMT3—a low-affinity ammonium transporter of the arbuscular mycorrhizal *Rhizophagus irregularis*. *Front. Plant Sci*. 7: 679.

Capaccio, L.C.M. and Callow, J.A. (1982) The enzymes of polyphosphate metabolism in vesicular–arbuscular mycorrhizas. *New Phytol.* 91: 81–91.

Conesa, A., Gotz, S., Garcia-Gomez, J.M., Terol, J., Talon, M. and Robles, M. (2005) Blast2GO: a universal tool for annotation, visualization and analysis in functional genomics research. *Bioinformatics* 21: 3674–3676.

Courty, P.E., Smith, P., Koegel, S., Redecker, D. and Wipf, D. (2015) Inorganic nitrogen uptake and transport in beneficial plant root-microbe interactions. *CRC Crit. Rev. Plant Sci*. 34: 4–16.

Cruz, C., Egsgaard, H., Trujillo, C., Ambus, P., Requena, N., Martins-Loucao, M.A., et al. (2007) Enzymatic evidence for the key role of arginine in nitrogen translocation by arbuscular mycorrhizal fungi. *Plant Physiol*. 144: 782–792.

Emms, D.M. and Kelly, S. (2015) OrthoFinder: solving fundamental biases in whole genome comparisons dramatically improves orthogroup inference accuracy. *Genome Biol*. 16: 157.

Ezawa, T. and Saito, K. (2018) How do arbuscular mycorrhizal fungi handle phosphate? New insight into fine-tuning of phosphate metabolism. *New Phytol*. 220: 1116–1121.

Fitter, A.H. (2006) What is the link between carbon and phosphorus fluxes in arbuscular mycorrhizas? A null hypothesis for symbiotic function. *New Phytol*. 172: 3–6.

Govindarajulu, M., Pfeffer, P.E., Jin, H., Abubaker, J., Douds, D.D., Allen, J.W., et al. (2005) Nitrogen transfer in the arbuscular mycorrhizal symbiosis. *Nature* 435: 819–823.

Harrison, M.J. and van Buuren, M.L. (1995) A phosphate transporter from the mycorrhizal fungus *Glomus versiforme*. *Nature* 378: 626–629.

Harrison, M.J., Dewbre, G.R. and Liu, J.Y. (2002) A phosphate transporter from *Medicago truncatula* involved in the acquisiton of phosphate released by arbuscular mycorrhizal fungi. *Plant Cell* 14: 2413–2429.

Helber, N., Wippel, K., Sauer, N., Schaarschmidt, S., Hause, B. and Requena, N. (2011) A versatile monosaccharide transporter that operates in the arbuscular mycorrhizal fungus *Glomus* sp. is crucial for the symbiotic relationship with plants. *Plant Cell* 23: 3812–3823.

Hijikata, N., Murase, M., Tani, C., Ohtomo, R., Osaki, M. and Ezawa, T. (2010) Polyphosphate has a central role in the rapid and massive accumulation of phosphorus in extraradical mycelium of an arbuscular mycorrhizal fungus. *New Phytol*. 186: 285–289.

Igiehon, N.O. and Babalola, O.O. (2017) Biofertilizers and sustainable agriculture: exploring arbuscular mycorrhizal fungi. *Appl. Microbiol. Biotechnol.* 101: 4871–4881.

Jabaji-Hare, S. (1988) Lipid and fatty acid profiles of some vesicular-arbuscular mycorrhizal fungi: contribution to taxonomy. *Mycologia* 80: 622–629.

Jiang, Y., Wang, W., Xie, Q., Liu, N., Liu, L., Wang, D., et al. (2017) Plants transfer lipids to sustain colonization by mutualistic mycorrhizal and parasitic fungi. *Science* 356: 1172–1175.

Jin, H., Pfeffer, P.E., Douds, D.D., Piotrowski, E., Lammers, P.J. and Shachar-Hill, Y. (2005) The uptake, metabolism, transport and transfer of nitrogen in an arbuscular mycorrhizal symbiosis. *New Phytol*. 168: 687–696.

Keymer, A., Pimprikar, P., Wewer, V., Huber, C., Brands, M., Bucerius, S.L., et al. (2017) Lipid transfer from plants to arbuscular mycorrhiza fungi. *Elife* 6: e29107.

Kikuchi, Y., Hijikata, N., Ohtomo, R., Handa, Y., Kawaguchi, M., Saito, K., et al. (2016) Aquaporin-mediated long-distance polyphosphate translocation directed towards the host in arbuscular mycorrhizal symbiosis: application of virus-induced gene silencing. *New Phytol.* 211: 1202–1208.

Kikuchi, Y., Hijikata, N., Yokoyama, K., Ohtomo, R., Handa, Y., Kawaguchi, M., et al. (2014) Polyphosphate accumulation is driven by transcriptome alterations that lead to near-synchronous and near-equivalent uptake of inorganic cations in an arbuscular mycorrhizal fungus. *New Phytol.* 204: 638–649.

Kim, D., Pertea, G., Trapnell, C., Pimentel, H., Kelley, R. and Salzberg, S.L. (2013) TopHat2: accurate alignment of transcriptomes in the presence of insertions, deletions and gene fusions. *Genome Biol.* 14: R36.

Kobae, Y., Tamura, Y., Takai, S., Banba, M. and Hata, S. (2010) Localized expression of arbuscular mycorrhiza-inducible ammonium transporters in soybean. *Plant Cell Physiol*. 51: 1411–1415.

Kobayashi, Y., Maeda, T., Yamaguchi, K., Kameoka, H., Tanaka, S., Ezawa, T., et al. (2018) The genome of *Rhizophagus clarus* HR1 reveals a common genetic basis for auxotrophy among arbuscular mycorrhizal fungi. *BMC Genomics* 19: 465.

Kuga, Y., Saito, K., Nayuki, K., Peterson, R.L. and Saito, M. (2008) Ultrastructure of rapidly frozen and freeze-substituted germ tubes of an arbuscular mycorrhizal fungus and localization of polyphosphate. *New Phytol.* 178: 189–200.

Lammers, P.J., Jun, J., Abubaker, J., Arreola, R., Gopalan, A., Bago, B., et al. (2001) The glyoxylate cycle in an arbuscular mycorrhizal fungus. Carbon flux and gene expression. *Plant Physiol*. 127: 1287–1298.

Li, X., George, E. and Marschner, H. (1991) Phosphorus depletion and pH decrease at the root–soil and hyphae–soil interfaces of VA mycorrhizal white clover fertilized with ammonium. *New Phytol.* 119: 397–404.

López-Pedrosa, A., González-Guerrero, M., Valderas, A., Azcón-Aguilar, C. and Ferrol, N. (2006) *GintAMT1* encodes a functional high-affinity ammonium transporter that is expressed in the extraradical mycelium of *Glomus intraradices*. *Fungal Genet. Biol.* 43: 102–110.

Luginbuehl, L.H., Menard, G.N., Kurup, S., Van Erp, H., Radhakrishnan, G.V., Breakspear, A., et al. (2017) Fatty acids in arbuscular mycorrhizal fungi are synthesized by the host plant. *Science* 356: 1175–1178.

Macdonald, R.M. and Lewis, M. (1978). The occurrence of some acid phosphatases and dehydrogenases in the vesicular-arbuscular mycorrhizal fungus *Glomus mosseae*. *New Phytol*. 80: 135–141.

Maeda, T., Kobayashi, Y., Kameoka, H., Okuma, N., Takeda, N., Yamaguchi, K., et al. (2018) Evidence of non-tandemly repeated rDNAs and their intragenomic heterogeneity in *Rhizophagus irregularis*. *Commun. Biol.* 1: 87.

Maldonado-Mendoza, I.E., Dewbre, G.R. and Harrison, M.J. (2001) A phosphate transporter gene from the extra-radical mycelium of an arbuscular mycorrhizal fungus *Glomus intraradices* is regulated in response to phosphate in the environment. *Mol. Plant Microbe Interact.* 14: 1140–1148.

Marleau, J., Dalpé, Y., St-Arnaud, M. and Hijri, M. (2011) Spore development and nuclear inheritance in arbuscular mycorrhizal fungi. *BMC Evol. Biol*. 11: 51.

Pearson, J.N. and Jakobsen, I. (1993) The relative contribution of hyphae and roots to phosphorus uptake by arbuscular mycorrhizal plants, measured by dual labelling with ^{32}P and ^{33}P. *New Phytol.* 124: 489–494.

Pérez-Tienda, J., Testillano, P.S., Balestrini, R., Fiorilli, V., Azcón-Aguilar, C. and Ferrol, N. (2011) GintAMT2, a new member of the ammonium transporter family in the arbuscular mycorrhizal fungus *Glomus intraradices*. *Fungal Genet. Biol*. 48: 1044–1055.

Pfeffer, P.E., Douds, D.D., Jr, Bécard, G. and Shachar-Hill, Y. (1999) Carbon uptake and the metabolism and transport of lipids in an arbuscular mycorrhiza. *Plant Physiol.* 120: 587–598.

Picelli, S., Björklund, Å.K., Faridani, O.R., Sagasser, S., Winberg, G. and Sandberg, R. (2013) Smart-seq2 for sensitive full-length transcriptome profiling in single cells. *Nat. Methods* 10: 1096–1098.

Picelli, S., Faridani, O.R., Björklund, Å.K., Winberg, G., Sagasser, S. and Sandberg, R. (2014) Full-length RNA-seq from single cells using Smart-seq2. *Nat. Protoc.* 9: 171–181.

Robinson, M.D., McCarthy, D.J. and Smyth, G.K. (2010) edgeR: a Bioconductor package for differential expression analysis of digital gene expression data. *Bioinformatics* 26: 139–140.

Roth, R. and Paszkowski, U. (2017) Plant carbon nourishment of arbuscular mycorrhizal fungi. *Curr. Opin. Plant Biol*. 39: 50–56.

Saito, M. (1995) Enzyme activities of the internal hyphae and germinated spores of an arbuscular mycorrhizal fungus, *Gigaspora margarita* Becker & Hall. *New Phytol.* 129: 425–431.

Sato, T., Ezawa, T., Cheng, W. and Tawaraya, K. (2015) Release of acid phosphatase from extraradical hyphae of arbuscular mycorrhizal fungus *Rhizophagus clarus*. *Soil Sci. Plant Nutr*. 61: 269–274.

Shachar-Hill, Y., Pfeffer, P.E., Douds, D., Osman, S.F., Doner, L.W. and Ratcliffe, R.G. (1995) Partitioning of intermediary carbon metabolism in vesicular-arbuscular mycorrhizal leek. *Plant Physiol.* 108: 7–15.

Sidoux-Walter, F., Pettersson, N. and Hohmann, S. (2004) The *Saccharomyces cerevisiae* aquaporin Aqy1 is involved in sporulation. *Proc. Natl. Acad. Sci. USA* 101: 17422–71427.

Sun, X., Chen, W., Ivanov, S., Maclean, A.M., Wight, H., Ramaraj, T., et al. (2019) Genome and evolution of the arbuscular mycorrhizal fungus *Diversispora epigaea* (formerly *Glomus versiforme*) and its bacterial endosymbionts. *New Phytol*. 221: 1556–1573.

Tang, N., San Clemente, H., Roy, S., Bécard, G., Zhao, B. and Roux, C. (2016) A Survey of the gene repertoire of *Gigaspora rosea* unravels conserved features among glomeromycota for obligate biotrophy. *Front. Microbiol*. 7: 233.

Tani, C., Ohtomo, R., Osaki, M., Kuga, Y. and Ezawa, T. (2009) ATP-dependent but proton gradient-independent polyphosphate-synthesizing activity in extraradical hyphae of an arbuscular mycorrhizal fungus. *Appl. Environ. Microbiol*. 75: 7044–7050.

Tian, C., Kasiborski, B., Koul, R., Lammers, P.J., Bucking, H. and Shachar-Hill, Y. (2010) Regulation of the nitrogen transfer pathway in the arbuscular mycorrhizal symbiosis: gene characterization and the coordination of expression with nitrogen flux. *Plant Physiol*. 153: 1175–1187.

Tisserant, E., Kohler, A., Dozolme-Seddas, P., Balestrini, R., Benabdellah, K., Colard, A., et al. (2012) The transcriptome of the arbuscular mycorrhizal fungus *Glomus intraradices* (DAOM 197198) reveals functional tradeoffs in an obligate symbiont. *New Phytol*. 193: 755–769.

Tisserant, E., Malbreil, M., Kuo, A., Kohler, A., Symeonidi, A., Balestrini, R., et al. (2013) Genome of an arbuscular mycorrhizal fungus provides insight into the oldest plant symbiosis. *Proc. Natl. Acad. Sci. USA* 110: 20117–20122.

Trépanier, M., Bécard, G., Moutoglis, P., Willemot, C., Gagné, S., Avis, T.J., et al. (2005) Dependence of arbuscular-mycorrhizal fungi on their plant host for palmitic acid synthesis. *Appl. Environ. Microbiol*. 71: 5341–5347.

Tsuzuki, S., Handa, Y., Takeda, N. and Kawaguchi, M. (2016) Strigolactone-induced putative secreted protein 1 is required for the establishment of symbiosis by the arbuscular mycorrhizal fungus *Rhizophagus irregularis*. *Mol. Plant Microbe Interact.* 29: 277–286.

van der Heijden, M.G.A., Bardgett, R.D. and van Straalen, N.M. (2008) The unseen majority: soil microbes as drivers of plant diversity and productivity in terrestrial ecosystems. *Ecol. Lett.* 11: 296–310.

van der Heijden, M.G.A., Klironomos, J.N., Ursic, M., Moutoglis, P., Streitwolf-Engel, R., Boller, T., et al. (1998) Mycorrhizal fungal diversity determines plant biodiversity, ecosystem variability and productivity. *Nature* 396: 69–72.

Viereck, N., Hansen, P.E. and Jakobsen, I. (2004) Phosphate pool dynamics in the arbuscular mycorrhizal fungus *Glomus intraradices* studied by *in vivo* ^{31}P NMR spectroscopy. *New Phytol.* 162: 783–794.

Walder, F., Boller, T., Wiemken, A. and Courty, P.E. (2016) Regulation of plants' phosphate uptake in common mycorrhizal networks: role of intraradical fungal phosphate transporters. *Plant Signal. Behav*. 11: e1131372.

Wewer, V., Brands, M. and Dörmann, P. (2014) Fatty acid synthesis and lipid metabolism in the obligate biotrophic fungus *Rhizophagus irregularis* during mycorrhization of *Lotus japonicus*. *Plant J.* 79: 398–412.

Yang, S.-Y., Grønlund, M., Jakobsen, I., Grotemeyer, M.S., Rentsch, D., Miyao, A., et al. (2012) Nonredundant regulation of rice arbuscular mycorrhizal symbiosis by two members of the *PHOSPHATE TRANSPORTER1* gene family. *Plant Cell* 24: 4236–4251.

Young, M.D., Wakefield, M.J., Smyth, G.K. and Oshlack, A. (2010) Gene ontology analysis for RNA-seq: accounting for selection bias. *Genome Biol.* 11: R14.

Zeng, T., Holmer, R., Hontelez, J., Te Lintel-Hekkert, B., Marufu, L., de Zeeuw, T., et al. (2018) Host- and stage-dependent secretome of the arbuscular mycorrhizal fungus *Rhizophagus irregularis*. *Plant J.* 94: 411–425.

Zhou, X., Lindsay, H. and Robinson, M.D. (2014) Robustly detecting differential expression in RNA sequencing data using observation weights. *Nucleic Acids Res*. 42: e91.